THE JOURNAL OF PHYSICAL CHEMISTRY B

Article

pubs.acs.org/JPCB

Are Ellipsoids Feasible Micelle Shapes? An Answer Based on a Molecular-Thermodynamic Model of Nonionic Surfactant Micelles

Jaisree Iyer and Daniel Blankschtein*

Department of Chemical Engineering, Massachusetts Institute of Technology, Cambridge, Massachusetts, 02139

Supporting Information

ABSTRACT: The existence of ellipsoidal micelles in aqueous solution has been debated in the literature. Although a number of experimental studies suggest that certain surfactants form ellipsoidal micelles, many theoretical studies have claimed that micelles with an ellipsoidal shape cannot exist. To shed light on this topic, in this paper, we develop a curvature-corrected, molecular-thermodynamic model for the free energy of micellization of nonionic surfactant biaxial ellipsoidal micelles. We subsequently use this model to evaluate the feasibility of forming ellipsoidal micelles, compared to forming spherical, spherocylindrical, and discoidal micelles, and conclude that ellipsoidal micelles can exist in solution. Utilizing the model developed here, we also establish theoretical limits on the size of the ellipsoidal micelles. These limits depend solely on the chemical structure of the surfactant molecule.

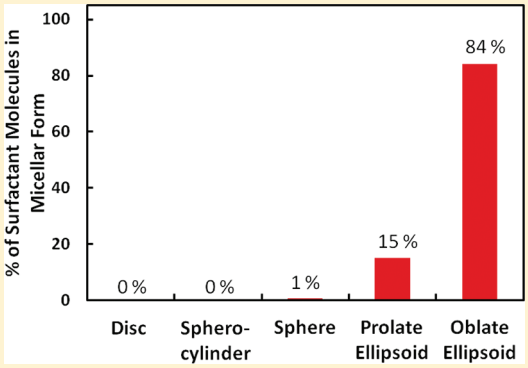

1. INTRODUCTION AND MOTIVATION

Surfactants are amphiphilic molecules that remain dispersed as monomers in aqueous solution at low concentrations. However, as the surfactant concentration increases beyond the critical micelle concentration (CMC), surfactants self-assemble to form aggregates called micelles. Micelles form in a variety of shapes and sizes depending on the chemical structure of the surfactant and the solution conditions, including surfactant concentration, salt concentration, and temperature. Several transport and thermodynamic properties of surfactant solutions are strongly affected by the shape and size distribution of the micelles. For example, the viscosity of an aqueous surfactant solution consisting of cylindrical micelles is significantly higher than that in the case of spherical or globular micelles.[1] The ability of an aqueous surfactant solution to solubilize hydrophobic solutes also depends on the shape and size distribution of the micelles.[2] Therefore, significant effort has been devoted to characterize the shape and size distribution of micelles in aqueous solution.[2,3]

In the literature on micelle shapes, there has been some controversy about the shape of globular micelles. Many experimental studies claim that some surfactants under certain solution conditions form ellipsoidal micelles. For example, for an aqueous solution of the nonionic surfactant *n*-dodecyl octaethylene glycol monoether, Tanford et al. compared the experimental viscosity and the experimental Stokes radii obtained from sedimentation velocity measurements to their respective theoretical predictions, and concluded that the micelles are oblate ellipsoidal (disk-like) in shape.[4] Kawaguchi et al. utilized X-ray scattering to show that nonionic short-chain fatty acid sucrose monoester surfactants (C_nSE; n = 10, 12, and 14) form oblate ellipsoidal micelles in aqueous solution.[5] Recently, experimental techniques like small-angle X-ray scattering and small-angle neutron scattering have been widely used to probe the structure of micelles.[3] For example, using small-angle X-ray scattering, Caetano et al. showed that the anionic surfactant sodium dodecyl sulfate in the presence of small amounts of Chlorpromazine (a clinical antipsychotic drug) forms prolate ellipsoidal micelles in aqueous solution.[6] Sarkar et al. showed that nonionic alkyl-propoxy-ethoxylate surfactants in the presence of alcohol cosolvents form oblate ellipsoidal micelles in aqueous solution.[7]

Several simulation studies have also suggested that surfactant micelles can have an ellipsoidal shape. For example, Bogusz et al. used molecular dynamics simulation to show that the nonionic surfactant, octyl glucoside, forms biaxial ellipsoidal micelles with an average eccentricity of 0.6.[8] Tieleman et al. used molecular dynamics simulation to show that the zwitterionic surfactant dodecylphosphocholine at a lower aggregation number forms ellipsoidal micelles having an average aspect ratio of 1.35.[9]

However, contrary to the experimental and simulations-based studies discussed above, several theoretical studies have refuted the premise that ellipsoids can be feasible micelle shapes. The most noteworthy of these studies is the seminal work of Israelachvili et al.[10] In response to the theoretical work of Tartar[11] and Tanford[12] where they studied the formation of ellipsoidal micelles once the surfactant molecules can no longer pack into spherical micelles, Israelachvili et al. invoked their packing criterion to claim that an ellipsoid cannot be an optimum micelle shape. They showed that, for an ellipsoidal micelle, the surface area per surfactant molecule varies

Received: February 8, 2012
Revised: March 29, 2012
Published: April 26, 2012

throughout the micelle surface, and is therefore different from the optimal surface area per surfactant molecule almost everywhere. As a result, from a free-energy viewpoint, an ellipsoidal shape can never be the optimal shape.[10] Subsequently, other authors also rejected the ellipsoid as a feasible micelle shape. In particular, Leibner and Jacobus claimed that ionic surfactants prefer to micellize in shapes with higher surface area per molecule in the head region. As a result, the spherocylinder shape is superior to the ellipsoid shape because spherocylinders have a higher surface area per molecule than those of prolate or oblate ellipsoids.[13] In another study, Taddei rejected the ellipsoidal shape based on the fact that ellipsoids have regions with high curvature (the polar region in a prolate ellipsoid and the equatorial region in an oblate ellipsoid), which will prevent the surfactant molecules from packing efficiently.[14,15]

Among the few studies on the theoretical modeling of the formation of ellipsoidal micelles, the most comprehensive one was undertaken by Halle et al. These authors calculated the free-energy change associated with the shape fluctuations of a spherical micelle that leads to the formation of an ellipsoidal micelle. Specifically, they accounted for the effect of the position-dependent curvature of the ellipsoidal shape on the free energy of micelle formation.[16] While their theoretical development of the electrostatic free energy of deformation was very thorough, Halle et al. did not account for the free-energy contributions arising from (i) the loss of conformational degrees of freedom of the surfactant tails in the micelle core, (ii) the steric interactions between the head groups of the surfactants, and (iii) the curvature dependence of the interfacial tension associated with the interfacial free energy of deformation.[16] Using their model, Halle et al. showed that, under certain conditions, both prolate and oblate ellipsoidal micelles can exist in aqueous solution. However, in their analysis, the authors only considered prolate ellipsoids, oblate ellipsoids, and spheres as possible shapes, leaving out cylinders or bilayers.

A few other studies in the literature on the structure of micelles include a molecular-thermodynamic model by Nagarajan and Ruckenstein[17] and a model based on shape fluctuations by Borkovec.[18] In both of these studies, the position-dependent curvature was not explicitly accounted for in the free-energy calculations. Instead, average geometrical properties of the ellipsoidal shape were used. On the basis of the limitations of the above modeling work, it is clear that, following the work by Israelachvili et al. on the shape of globular micelles, there has not been a rigorous theoretical study on ellipsoidal micelles that analyses the effect of the position-dependent curvature on the free energy of micelle formation, including evaluating the feasibility that ellipsoidal micelles can form in an aqueous surfactant solution relative to other commonly formed micelle shapes, including spheres, spherocylinders, and discs. With this need in mind, in this paper, we first develop a theoretical framework based on molecular thermodynamics to calculate the free energy associated with forming nonionic prolate and oblate ellipsoidal micelles. Subsequently, in the context of our theoretical description, we provide a rigorous answer to the question: are ellipsoids feasible micelle shapes?

Our paper is organized as follows. A brief overview of the molecular-thermodynamic framework used here is presented in section 2.1. The theoretical development of the different free-energy expressions for biaxial ellipsoidal micelles is presented in sections 2.2−2.4. Results and discussions, including evaluating the feasibility of forming biaxial ellipsoidal micelles relative to other commonly formed micelle shapes, are presented in section 3. Finally, our conclusions are summarized in section 4. Additional useful information is provided in the Supporting Information.

2. THEORY

2.1. Review of the Molecular-Thermodynamic Framework. The molecular-thermodynamic framework used here blends the thermodynamics of a micellar solution with a molecular-level description of the free energy of micellization, which is a quantitative measure of the tendency of a surfactant molecule to transfer from the monomeric state to the micellar state. Given the chemical structure of a surfactant and the solution conditions, this framework can predict several micellization properties, including the critical micelle concentration, and the micelle shape and size in solution, without using any fitting parameters.[19]

Using concepts from thermodynamics, the free energy, G, of an aqueous surfactant solution containing N_S surfactant molecules dispersed in N_W water molecules can be written as follows:[20]

$$G = N_W\mu_{W,0} + N_1\mu_{1,0} + \sum_{n>1} N_n n g_{mic} + N_W kT \ln X_W + N_1 kT \ln X_1 + \sum_{n>1} N_n kT \ln X_n \quad (1)$$

where $\mu_{W,0}$ is the chemical potential of pure water, $\mu_{1,0}$ is the chemical potential of a surfactant monomer at infinite dilution, N_1 is the number of surfactant monomers, N_n is the number of surfactant micelles with an aggregation number n, g_{mic} is the free energy of micellization per surfactant molecule and is a function of the characteristics of the micelle, including its shape and size, k is the Boltzmann constant, T is the absolute temperature, and X_i denotes the mole fraction of component i (i = 1, W, and n), and is defined as $X_i = N_i/(N_W + N_S)$.[21] Note that the number of monomers and the number of micelles are related to the total number of surfactant molecules added in solution through the mass balance equation:

$$N_1 + \sum_{n>1} nN_n = N_S \quad (2)$$

Minimizing the free energy of the surfactant solution defined in eq 1, subject to the mass balance constraint stated in eq 2, yields the following expression for X_n:[22]

$$X_n = \frac{1}{e}\left(\frac{X_1}{\exp\left(\frac{g_{mic}}{kT} - 1\right)}\right)^n \quad (3)$$

Note that the concentration of micelles of aggregation number n depends not only on n but also on other characteristics of the micelle, namely, the micelle shape and size for a nonionic surfactant. This is because X_n is a function of g_{mic} which, in turn, is a function of the micelle shape and size. Therefore, the concentration of every micelle type can be calculated by substituting the free energy of micellization associated with that micelle type in eq 3. As stated above, the free energy of micellization is the free-energy change experienced by a surfactant molecule as it transfers from the monomeric state to the micellar state. Since free energy is a state function, we can construct a convenient hypothetical path to calculate the free energy of micellization. For a nonionic surfactant, g_{mic} can be broken down as follows:[19]

dx.doi.org/10.1021/jp3012975 | J. Phys. Chem. B 2012, 116, 6443−6454

$$g_{mic} = g_{tr} + g_{int} + g_{pack} + g_{st} \quad (4)$$

where g_{tr} is the transfer free energy per molecule, g_{int} is the interfacial free energy per molecule, g_{pack} is the packing free energy per molecule, and g_{st} is the steric free energy per molecule. Equation 4 can be obtained by conceiving a hypothetical path in which one first breaks the bond connecting the surfactant head and tail to separate the head from the tail. Subsequently, one transfers the tail from an aqueous environment to a bulk tail-like (oil) phase. The free-energy change associated with this step is the transfer free energy, and can be expressed in terms of the aqueous solubility of the tail, S, as follows:[19,23]

$$g_{tr} = kT \ln S \quad (5)$$

Following that, one re-establishes the contact between the tail phase and water by forming a drop from the tail phase. The free-energy change associated with this step is known as the interfacial free energy, and is modeled as follows:[19]

$$g_{int} = \sigma(a - a_0) \approx \sigma_0(1 - 2c\delta)(a - a_0) \quad (6)$$

where σ is the curvature-corrected interfacial tension between water and the oil drop, a is the surface area per molecule, and a_0 is the surface area of the oil drop that is shielded from contact with water due to the physical connection between the surfactant head and tail. Note that, in eq 6, we have used Tolman's correction to estimate the interfacial tension for a curved interface, σ, using the curvature of the interface, c, the Tolman distance, δ, and the interfacial tension across a flat interface, σ_o.[24] In addition, note that the curvature of the interface, c, depends on the shape of the micelle. For example, for the three regular shapes, spheres, infinite cylinders, and infinite bilayers, $c = 1/r$, $1/2r$, and 0, respectively, where r is the radius of the sphere or infinite cylinder.

At this point, we recognize that the oil drop does not mimic the micelle core precisely because the surfactant tails are subject to stricter conformational constraints in the micelle core than in the oil drop. Indeed, in the micelle core, one end of the surfactant tails has to be tethered at the micelle core–water interface to maintain the physical connection between the surfactant head and tail. The free-energy change associated with constraining the surfactant tails to mimic the micelle core is called the packing free energy per molecule, g_{pack}. It is calculated based on a mean-field, statistical-mechanical method developed by Ben-Shaul et al.[25] For details, the interested reader is referred to the paper by Srinivasan and Blankschtein.[26]

Finally, the only remaining step to form the micelle is to rejoin the surfactant head and tail. Since the rejoining process involves the localization of several finite-sized surfactant heads in a finite region, there is a free-energy penalty associated with this step known as the steric free energy per molecule, g_{st}. This is calculated by estimating the free-energy change associated with the excluded-volume interactions between the surfactant heads. Specifically,[19]

$$g_{st} = -kT \ln\left(1 - \frac{a_h}{a}\right) \quad (7)$$

where a_h is the area of the surfactant head. Adding all the free-energy contributions, namely, g_{tr}, g_{int}, g_{pack}, and g_{st}, yields g_{mic} as stated in eq 4.

Implementation of the g_{mic} model in the case of the free energy of micellization of ellipsoidal micelles is particularly challenging compared to its implementation in the case of the basic micelle shapes like spheres, infinite cylinders, and infinite bilayers. This is due to the position-dependent curvature associated with ellipsoids. For example, variables like the surface area per molecule, a, and the curvature, c, vary throughout the ellipsoid surface instead of having a unique value as is the case for spheres, infinite cylinders, and infinite bilayers. Therefore, developing a model to calculate g_{mic} in the case of ellipsoidal micelles involves an additional new step which blends concepts of differential geometry with the models described above. This new step is discussed in the following three sections.

2.2. Interfacial Free Energy for Biaxial Ellipsoidal Micelles.

As shown in eq 6, the interfacial free energy per molecule, g_{int}, can be modeled as the product of the curvature-corrected interfacial tension between water and the micelle core, σ, and the surface area of the micelle core per surfactant molecule that is exposed to water. Using Tolman's theory, the curvature-corrected interfacial tension can be modeled as follows:[19,24]

$$\sigma \approx \sigma_0(1/(1 + 2c\delta)) \approx \sigma_0(1 - 2c\delta) \quad (8)$$

In obtaining eq 8, we have used a Taylor series expansion to linearize $1/(1 + 2c\delta)$, which has also been used to obtain eq 6. Note that, in the limit $2c\delta \ll 1$, this linearization does not introduce significant errors. As was stated earlier, geometrical properties like the mean curvature and the surface area per molecule vary along an ellipsoidal surface. As a result, it is expected that the interfacial free energy per molecule, and in turn the micellization free energy per molecule, will vary along the ellipsoidal surface. To calculate the concentration of a micelle of a given shape and size using eq 3, we require a single value of g_{mic} instead of a distribution of g_{mic} values varying along the ellipsoidal surface. As a result, an appropriate average free energy of micellization is required, which can be calculated by computing average values for g_{int}, g_{pack}, and g_{st}. To calculate an average interfacial free energy per molecule, we first calculate the *extensive* interfacial free energy, G_{int}, for the ellipsoidal micelle, which when divided by the micelle aggregation number yields an average g_{int}. Note that this method of calculating the average g_{int} is different from calculating the average g_{int} using an average surface area per molecule and an average value for the mean curvature. This is because g_{int} and the other free-energy contributions have a nonlinear dependence on the ellipsoidal geometrical properties, including the surface area per molecule and the mean curvature.

To obtain G_{int}, we first derive an expression for the local differential interfacial free-energy penalty, $dG_{int,local}$, as a function of the position along the ellipsoidal surface, and then integrate this expression over the entire surface. Similar to eq 6, the differential interfacial free energy can be written as follows:

$$dG_{int,local} = \sigma_0(1 - 2c\delta)(dA - a_0 \cdot dn) \quad (9)$$

where dn denotes the differential number of molecules associated with the differential area dA, and therefore, $a_0 \cdot dn$ denotes the differential shielding area. Since the micelle core is assumed to be fluid-like, it has a constant density. This suggests that dn can be written as follows:

$$dn = (n/V)\, dV \quad (10)$$

where dV and V are the differential volume and the total volume of the micelle core, respectively.

To define geometrical parameters like the mean curvature, c, and the differential area, dA, we introduce the following parametrization of the ellipsoidal surface:

dx.doi.org/10.1021/jp3012975 | J. Phys. Chem. B 2012, 116, 6443–6454

$$x = p \cos u \sin v$$
$$y = p \sin u \sin v, \quad 0 \le u < 2\pi \text{ and } 0 \le v \le \pi$$
$$z = q \cos v \tag{11}$$

where p and q are the lengths of the two different semiaxes and the angles u and v are similar to the azimuth and polar angles used in the spherical coordinate system. The angles u and v associated with an arbitrary point on the ellipsoidal surface are shown in Figure 1. Note that, for prolate ellipsoids, $q > p$, while, for oblate ellipsoids, $q < p$. Using the Jacobian associated with the above coordinate system, the differential volume, dV, can be written as follows:

$$dV = \frac{p^2 q}{3} \sin v \, du \, dv \tag{12}$$

Using the first and second fundamental forms[27] associated with the parametrization in eq 11, one can write the mean curvature and differential area for ellipsoids as follows:

$$c = \frac{q(p^2 + p^2 \cos^2 v + q^2 \sin^2 v)}{2p(p^2 \cos^2 v + q^2 \sin^2 v)^{3/2}} \tag{13}$$

$$dA = p \sin v \sqrt{p^2 \cos^2 v + q^2 \sin^2 v} \, du \, dv \tag{14}$$

Substituting eqs 10, 12, 13, and 14 in eq 9 yields

$$dG_{int,local} = \sigma_0 p \sin v \left(1 - \frac{q}{p} \frac{(p^2 + p^2 \cos^2 v + q^2 \sin^2 v)}{(p^2 \cos^2 v + q^2 \sin^2 v)^{3/2}} \delta\right) \left(\sqrt{p^2 \cos^2 v + q^2 \sin^2 v} - a_0 \frac{n}{V} \frac{pq}{3}\right) du \, dv \tag{15}$$

Integrating eq 15 and then dividing the integrated expression by the aggregation number, n, of the ellipsoidal micelle yields the average interfacial free energy per molecule, g_{int}. Specifically,

$$g_{int} = \begin{cases} \sigma_0 \left(\frac{A}{n} - a_0 - \frac{4\pi q \delta}{n} \left(\frac{\left(\frac{p}{q}\right)^2}{\sqrt{\left(\frac{p}{q}\right)^2 - 1}} \tan^{-1} \sqrt{\left(\frac{p}{q}\right)^2 - 1} + 1 \right) + \frac{2\delta A}{3V} a_0 \right) & \text{if } p > q \\ \sigma_0 \left(\frac{A}{n} - a_0 - \frac{4\pi q \delta}{n} \left(\frac{\left(\frac{p}{q}\right)^2}{\sqrt{1 - \left(\frac{p}{q}\right)^2}} \ln \left| \frac{q}{p} + \sqrt{\left(\frac{q}{p}\right)^2 - 1} \right| + 1 \right) + \frac{2\delta A}{3V} a_0 \right) & \text{if } p < q \end{cases} \tag{16}$$

In the limit when p/q tends to 1, one can show that eq 16 reduces to eq 6 with $p = q = 1/c$.

2.3. Packing Free Energy for Biaxial Ellipsoidal Micelles. Our approach to calculate the packing free energy is based on a mean-field, statistical-mechanical method developed by Ben-Shaul et al.[25] In this approach, the free energy of the packed state, g_{conf}, is given by

$$g_{conf} = \sum_{\alpha, v_{surface}} P(\alpha, v_{surface}) \varepsilon(\alpha) + kT \sum_{\alpha, v_{surface}} P(\alpha, v_{surface}) \ln P(\alpha, v_{surface}) \tag{17}$$

where α denotes the chain conformation, $v_{surface}$ is the location on the ellipsoidal surface where the surfactant tail is tethered, $\varepsilon(\alpha)$ is the energy associated with conformation α, and $P(\alpha, v_{surface})$ is the probability of finding the chain in conformation α when it is tethered at the location $v_{surface}$ on the ellipsoidal surface. Note that the chain conformations depend on (i) the external orientation of the chain with respect to the micelle core−water interface and (ii) the internal conformation of the chain which involves the bond sequences of the chains. Most commonly used surfactants have linear hydrocarbon or fluorocarbon tails. For these surfactant tails, the bond lengths and bond angles are fixed at the equilibrium values, and the dihedral angles are sampled based on the rotational isomeric state (RIS) model.[28,29] Note that the model for calculating the packing free energy is not limited to just linear hydrocarbon and fluorocarbon chains. However, in this paper, we have only considered surfactants with linear hydrocarbon or fluorocarbon tails because these are the most commonly found surfactant tails.

To use eq 17, one needs an expression for $P(\alpha, v_{surface})$. In an unconstrained problem, P would be a function of only the energy of the chain conformation α. However, due to the constraints imposed on the micelle core, $P(\alpha, v_{surface})$ is governed not only by the energy of the conformation but also by the constraints imposed on the system. The three constraints imposed on the micelle core require the following: (i) no part of the chain can be on the water side of the micelle core−water interface, (ii) the end of the tail which is connected to the head is tethered at the interface, and (iii) the entire micelle core volume is occupied by the chains. The first two constraints limit the types of conformations that the chain can adopt; that is, any conformation that violates the first two constraints has a zero probability of being realized. The third constraint can be stated mathematically as follows:

$$\sum_{\alpha, v_{surface}} P(\alpha, v_{surface}) \phi(x, v, \alpha, v_{surface}) = V(x, v) \tag{18}$$

where x and v denote the layer and cell location, as illustrated in Figure 2, $\phi(x, v, \alpha, v_{surface})$ is the volume occupied by a chain, in conformation α and tethered at $v_{surface}$, in cell v of layer x, and $V(x, v)$ is the volume available per surfactant molecule in cell v of layer x. The expression for $P(\alpha, v_{surface})$ is obtained by minimizing g_{conf} subject to the constraint given in eq 18. The resulting expression for $P(\alpha, v_{surface})$ is given by[26]

dx.doi.org/10.1021/jp3012975 | J. Phys. Chem. B 2012, 116, 6443−6454

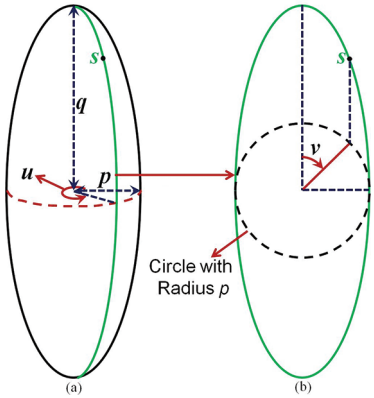

Figure 1. Schematic of a prolate ellipsoid illustrating the parametrization introduced in eq 11. The figure shows the definitions of the angles u and v associated with the point s. In part a, we present a three-dimensional view of a prolate ellipsoid, while in part b, we present the two-dimensional cross-sectional view associated with the green curve in part a.

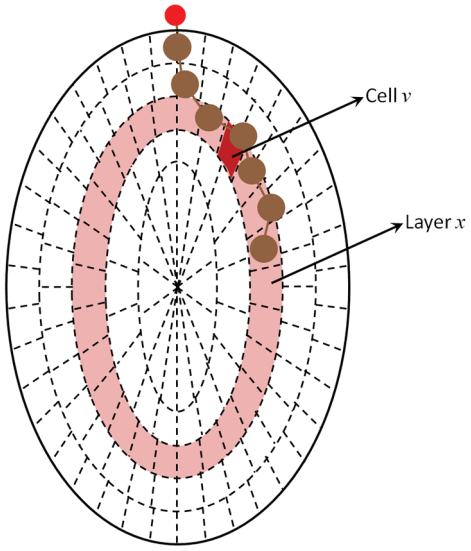

Figure 2. Schematic showing the division of the ellipsoidal volume into layers and cells to aid in the calculation of the packing free energy. The red circle is a dummy group representing the surfactant head, while the brown circles represent the surfactant tail groups.

$$P(\alpha, v_{surface}) = \frac{\exp[-\beta\varepsilon(\alpha) - \beta\sum_{x,v}\pi(x, v)\phi(x, v, \alpha, v_{surface})]}{\sum_{\alpha,v_{surface}}\exp[-\beta\varepsilon(\alpha) - \beta\sum_{x,v}\pi(x, v)\phi(x, v, \alpha, v_{surface})]} \quad (19)$$

where $\beta = (kT)^{-1}$ and $\pi(x,v)$ is the Lagrange multiplier associated with the constraint given in eq 18. Note that $\pi(x, v)$ may be interpreted as the pressure that has to be exerted to force the chains to occupy the entire micelle core volume. Equations 18 and 19 can be solved self-consistently for $\pi(x, v)$, and subsequently, eq 17 can be used to compute the free energy of the packed state.

The computational cost of calculating the packing free energy for a biaxial ellipsoidal micelle can be reduced by taking advantage of the symmetry features associated with this shape. Specifically, a biaxial ellipsoid has an axis of symmetry and a plane of symmetry that is perpendicular to the axis of symmetry. These symmetry features can be used to reduce the three-dimensional packing problem to a two-dimensional problem, thereby reducing the number of cells and the number of sampling points required to accurately estimate g_{pack}. However, while using symmetry features, one has to carefully assign appropriate weights to these fewer sampling locations based on the likelihood that a surfactant chain is present at a location which is geometrically equivalent to the sampling location. Additional details about the model used here to calculate the packing free energy are provided in the Supporting Information.

Note that, for the regular shapes (spheres, infinite cylinders, and infinite bilayers), the packing free energy can be calculated without dividing the layers into cells. This follows because, for these three shapes, different cells in the same layer are geometrically identical. Similarly, since all locations on the surface of a sphere, an infinite cylinder, or an infinite bilayer are identical, it suffices to sample all the chain conformations only at one location. Using these simplifications, one can show that eqs 17−19 reduce to the packing equations used by Srinivasan and Blankschtein.[26]

The final piece in calculating the packing free energy requires the calculation of g_{conf} for the free oil-drop state, $g_{conf,free}$. This can be obtained by lifting all the constrains, or in other words, by setting $\pi = 0$ in eq 19.[26] This yields

$$g_{conf,free} = -kT \ln \sum_{\alpha,v_{surface}} \exp(-\varepsilon(\alpha)/kT) \quad (20)$$

Using eqs 17 and 20, one can calculate the packing free energy as follows:

$$g_{pack} = g_{conf} - g_{conf,free} \quad (21)$$

It is clear that the computation of the packing free energy using the above method requires a significant amount of computational memory. Therefore, using the packing free energy data, we generate a polynomial fit that relates the packing free energy to the micelle characteristics, namely, to the micelle shape and size, and use this polynomial function for subsequent calculations of g_{mic}.[30]

2.4. Steric Free Energy for Biaxial Ellipsoidal Micelles.

The method used to calculate the steric free energy for an ellipsoidal micelle is very similar to the method used to compute the interfacial free energy. In summary, we first use concepts from differential geometry to derive expressions for local geometric features. These are shown in eqs 12−14. Using these expressions, we subsequently derive an equation for the differential steric free energy, $dG_{st,local}$, which is then integrated over the ellipsoidal surface and divided by the aggregation number of the ellipsoidal micelle to yield g_{st}. The key equations are summarized below:

$$dG_{st,local} = -dn\cdot kT \ln\left(1 - \frac{a_h\cdot dn}{dA}\right) = -\left(\frac{n}{V}\,dV\right)\cdot kT \times \ln\left(1 - \frac{a_h\cdot\left(\frac{n}{V}\right)dV}{dA}\right)$$

$$= -\frac{nkT}{4\pi}\ln\left(1 - \frac{na_h}{4\pi p\sqrt{p^2\cos^2 v + q^2\sin^2 v}}\right) \times \sin v\, dv\, du \quad (22)$$

dx.doi.org/10.1021/jp3012975 | J. Phys. Chem. B 2012, 116, 6443−6454

$$g_{st} = \frac{\int dG_{st,local}}{n} = \int_{u=0}^{u=2\pi}\int_{v=0}^{v=\pi} -\frac{nkT}{4\pi n} \times \ln\left(1 - \frac{na_h}{4\pi p\sqrt{p^2\cos^2 v + q^2\sin^2 v}}\right)\sin v\, dv\, du$$

$$= -\frac{k_B T}{2}\int_{v=0}^{v=\pi} \ln\left(1 - \frac{na_h}{4\pi p\sqrt{p^2\cos^2 v + q^2\sin^2 v}}\right) \times \sin v\, dv \quad (23)$$

Since the integral in eq 23 cannot be evaluated analytically, we use the Gaussian quadrature numerical integration technique to calculate the steric free energy for a biaxial ellipsoid.

3. RESULTS AND DISCUSSION

In this section, we first systematically elucidate the effect of surfactant molecular descriptors and micelle parameters on the different free-energy contributions associated with the micellization free energy of biaxial ellipsoidal micelles introduced in section 2. Subsequently, we apply this understanding to assess the feasibility of the biaxial ellipsoidal shape as a micelle shape in comparison with other micelle shapes, namely, spherical, spherocylindrical, and discoidal micelles. As stated in section 1, in this paper, we limit our study to nonionic surfactants having linear hydrocarbon or fluorocarbon tails because these are the most commonly encountered surfactant tails. In addition, typical fluorocarbon surfactants are short, and therefore, our focus here is on short chain surfactants. The model presented here can be readily extended to other nonionic surfactants. However, the computational memory associated with calculating the packing free energy per molecule will increase with the increase in the number of carbon atoms in the surfactant tail.

3.1. Results for the Interfacial Free Energy of Biaxial Ellipsoidal Micelles. A plot of the variation of the local interfacial free energy per molecule, $g_{int,local}$, along the surface of a prolate ellipsoid is shown in Figure 3. The figure is obtained

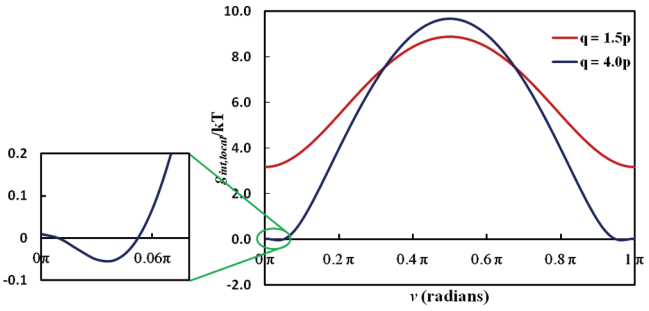

Figure 3. Variation of the local interfacial free energy per molecule, $g_{int,local}$, as a function of the angle v for a prolate ellipsoidal micelle.

by dividing eq 15 by eq 10 for a prolate ellipsoidal micelle core formed by a six-carbon fluorocarbon tail with a tail volume of 292.0 Å^3, σ_0 = 55.0 dyn/cm, δ = 1.28 Å, T = 298.15 K, and a_0 = 29.8 Å^2, which is equal to the cross-sectional area of a CF_2-CF_2 bond in a fluorocarbon chain, and p = 7.40 Å, which is equal to 95% of the fully extended length of the six-carbon fluorocarbon tail. This corresponds to aggregation numbers of 9 and 23 for the red and blue curves, respectively. Figure 3 shows that $g_{int,local}$ is highest at $v = \pi/2$, and decreases close to the poles of the prolate ellipsoid located at v = 0 and π. In fact, at the higher aspect ratio considered here (q/p = 4.0), $g_{int,local}$ becomes negative near the poles (see the zoomed in view of the blue curve corresponding to q/p = 4.0 in Figure 3). The interfacial free energy at high aspect ratios is negative because the amount of shielding in the polar region exceeds the available surface area. Since this is not physically realizable, it merely suggests that a prolate ellipsoid with such a high aspect ratio is not a feasible micelle shape. From the expression for $dG_{int,local}$ in eqs 9 and 15, it follows that the interfacial free energy will be positive if

$$\sqrt{p^2\cos^2 v + q^2\sin^2 v} - a_0\frac{n}{V}\frac{pq}{3} > 0, \qquad 0 \le v \le \pi$$

$$\Rightarrow \begin{cases} p - a_0\dfrac{n}{nV_{tail}}\dfrac{pq}{3} > 0, & 0 \le v \le \pi, \quad p < q \\ q - a_0\dfrac{n}{nV_{tail}}\dfrac{pq}{3} > 0, & 0 \le v \le \pi, \quad p > q \end{cases}$$

$$\Rightarrow \begin{cases} q < \dfrac{3V_{tail}}{a_0}, & p < q \\ p < \dfrac{3V_{tail}}{a_0}, & p > q \end{cases} \quad (24)$$

where V_{tail} is the volume of the surfactant tail. Note that $dG_{int,local}$ can also be negative if $1 < 2c\delta$ (which corresponds to negative values of the curvature corrected interfacial tension). However, for typical sizes of surfactant micelles, such a scenario is not encountered.

On the basis of eq 24, it follows that knowledge of the structure of the surfactant tail is sufficient to establish a theoretical limit on the size of feasible ellipsoidal micelles using the curvature-corrected model presented here. Note that this result is consistent with the qualitative claims made in a few theoretical studies on ellipsoidal micelles that highly elongated ellipsoidal micelles are not feasible micelle shapes.[14,15]

For the same six-carbon fluorocarbon tail, the variation of the average interfacial free energy per molecule, g_{int}, as a function of the size of the ellipsoidal micelle is shown in Figure 4. For the solid red and blue curves, the aggregation number increases

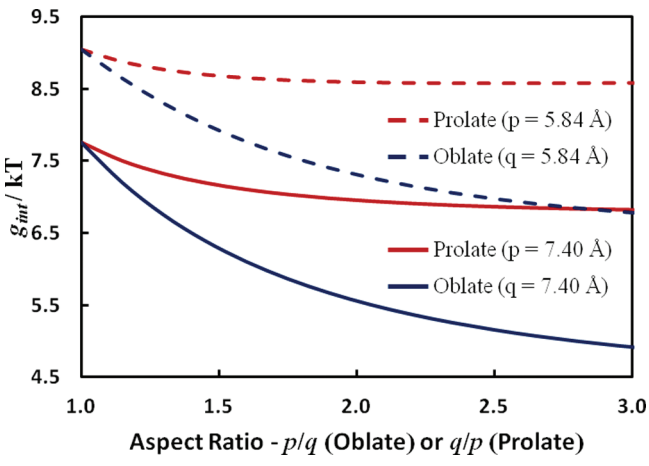

Figure 4. Variation of g_{int} with the aspect ratio of prolate ellipsoidal micelles and oblate ellipsoidal micelles. The dashed lines and the solid lines correspond to ellipsoidal micelles having a semiminor axis length equal to 75 and 95% of the six-carbon fluorocarbon tail length, respectively.

dx.doi.org/10.1021/jp3012975 | J. Phys. Chem. B 2012, 116, 6443−6454

from 6 to 17 and 52, respectively, as one moves from left to right along the aspect ratio axis. Similarly, for the dashed red and blue curves, the aggregation number increases from 3 to 9 and 26, respectively, as one moves from left to right along the aspect ratio axis. Figure 4 shows that, for the same semiminor axis length and aspect ratio, an oblate ellipsoidal micelle (the two blue curves) has a significantly lower g_{int} compared to a prolate ellipsoidal micelle (the two red curves). This difference follows because, for the same semiminor axis length and aspect ratio, an oblate ellipsoid has a lower surface area per molecule than a prolate ellipsoid. Similarly, g_{int} decreases as the semiminor axis length increases, or as the aspect ratio increases. This trend again follows because an increase in the semiminor axis length, or in the aspect ratio, leads to a decrease in the surface area per molecule.

The final plot in this section, shown in Figure 5, compares g_{int} for an ellipsoidal micelle core formed by fluorocarbon

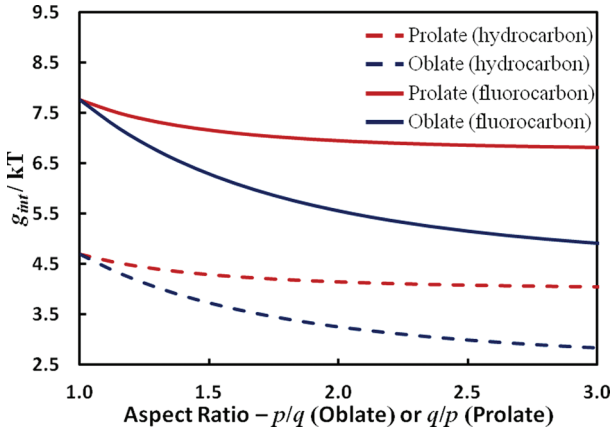

Figure 5. Variation of g_{int} with the aspect ratio of prolate ellipsoidal micelles and oblate ellipsoidal micelles. The dashed lines and the solid lines correspond to ellipsoidal micelle cores formed by hydrocarbon chains and fluorocarbon chains, respectively.

chains (the solid curves) with g_{int} for an ellipsoidal micelle core formed by hydrocarbon chains (the dashed curves). The molecular descriptors associated with the hydrocarbon tail are V_{tail} = 188.8 Å^3, σ_0 = 50.46 dyn/cm, δ = 1.19 Å, T = 298.15 K, and a_0 = 21.0 Å^2, which is equal to the cross-sectional area of a CH_2−CH_2 bond in a hydrocarbon chain. The semiminor axis for both types of biaxial ellipsoidal micelles is fixed at 95% of the length of the six-carbon fluorocarbon or hydrocarbon tail. This corresponds to 7.40 Å for the fluorocarbon tail and to 7.28 Å for the hydrocarbon tail. Due to the reduced tail volume and semiminor axis length, the aggregation numbers for the hydrocarbon-based surfactant vary between 9 and 77. Figure 5 shows that, for both the prolate ellipsoidal micelle shape (the red curves) and the oblate ellipsoidal micelle shape (the blue curves), the core formed by hydrocarbon chains has a lower g_{int} compared to that formed by fluorocarbon chains. This follows because a hydrocarbon chain has a much lower tail volume (188.8 Å^3) compared to its fluorocarbon counterpart (292.0 Å^3). Therefore, for the same surface area, a larger number of hydrocarbon chains can be accommodated in the micelle core volume, leading to a lower interfacial free energy *per molecule*.

3.2. Results for the Packing Free Energy of Biaxial Ellipsoidal Micelles. The packing polynomials for different fluorocarbon and hydrocarbon chains used in this study are tabulated in the Supporting Information. Using these polynomial functions, we calculated the packing free energy per molecule, g_{pack}, for a six-carbon fluorocarbon tail packed in prolate and oblate ellipsoidal micelle cores of different sizes. The curves are shown in Figure 6. The red and blue curves

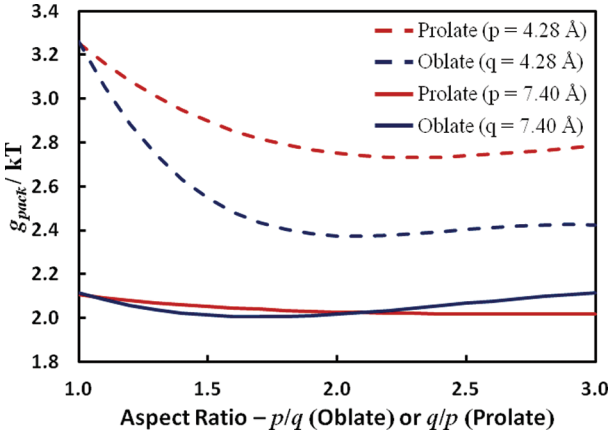

Figure 6. Variation of g_{pack} with the aspect ratio of prolate ellipsoidal micelles and oblate ellipsoidal micelles. The dashed lines and the solid lines correspond to ellipsoidal micelle cores having a semiminor axis length equal to 55 and 95% of the length of the fluorocarbon tail, respectively.

correspond to g_{pack} for prolate and oblate ellipsoidal micelle cores, respectively, while the dashed and solid curves correspond to semiminor axis lengths equal to 55 and 95% of the surfactant tail length which corresponds to 4.28 and 7.40 Å, respectively. Inspection of the dashed curves shows that, for small semiminor axis lengths, g_{pack} decreases as the aspect ratio increases and plateaus off at higher aspect ratios. This follows because, when both semiaxis lengths are small, the ellipsoidal surface has a very high curvature. Consequently, the chains have to twist considerably to remain completely in the interior of the ellipsoid, leading to many gauche defects, and therefore to higher g_{pack} values. However, as the aspect ratio increases, more volume is available to the chains in the ellipsoid. This allows them to adopt several other chain conformations which were not allowed at smaller aspect ratios, thereby resulting in a lower value of g_{pack}. This trend is observed for both prolate and oblate ellipsoidal micelles, as reflected in the dashed curves in Figure 6. At higher aspect ratios, the decrease in g_{pack} due to the increase in the volume of the ellipsoidal core and the increase in g_{pack} due to the increase in curvature at the equatorial region (for oblate ellipsoids) or the polar region (for prolate ellipsoids) seem to offset each other, resulting in the flattening of the dashed curves.

An increase in the semiminor axis length (the solid curves) leads to a decrease in g_{pack} for both prolate and oblate ellipsoidal micelles. This follows because an increase in the semiminor axis length leads to a decrease in the curvature, which in turn leads to less stringent restrictions on the types of conformations that a chain can adopt, and therefore to a lower g_{pack}. However, at large semiminor axis lengths, the trend for g_{pack} as a function of the aspect ratio for a prolate ellipsoidal micelle (the solid red curve) differs from that for an oblate ellipsoidal micelle (the solid blue curve). Specifically, for a prolate ellipsoid, g_{pack} does not change significantly with an increase in the aspect ratio in spite of the increase in curvature at the poles of the prolate ellipsoid. This follows because not many molecules occupy the poles of the prolate ellipsoid, and

dx.doi.org/10.1021/jp3012975 | J. Phys. Chem. B 2012, 116, 6443−6454

therefore, the polar region does not contribute greatly to the value of g_{pack}. In contrast, for an oblate ellipsoid, g_{pack} increases with the aspect ratio. As the aspect ratio of an oblate ellipsoid increases, the curvature at the equatorial region also increases. Therefore, molecules occupying the equatorial region are not only subjected to stringent conformational constraints due to the high curvature but also need to stretch out (adopt almost an all-trans conformation) to fill out the volume in the center of the ellipsoid. Since many molecules occupy the equatorial region, their loss of conformational degrees of freedom due to these two requirements leads to an increase in g_{pack}.

Finally, in Figure 7, we compare the difference between the g_{pack} values for fluorocarbon chains (the solid curves) and

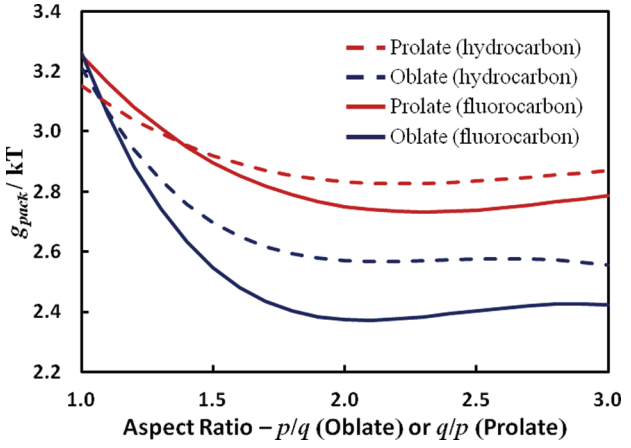

Figure 7. Variation of g_{pack} with the aspect ratio of prolate ellipsoidal micelles and oblate ellipsoidal micelles. The dashed lines and the solid lines correspond to ellipsoidal micelle cores having hydrocarbon chains and fluorocarbon chains, respectively.

hydrocarbon chains (the dashed curves). All the curves in Figure 7 correspond to a six-carbon chain. The energy of a conformation for the hydrocarbon chain is calculated using the three-state rotational isomeric state (RIS) model for linear alkanes,[28,29] and that for the fluorocarbon chain is calculated using the three-state RIS model developed by Bates and Stockmayer.[31] Figure 7 shows that a hydrocarbon chain has a lower g_{pack} value than its fluorocarbon analogue when the ellipsoid is small (i.e., has relatively higher curvature). This trend is seen in both prolate and oblate ellipsoidal micelles; however, this trend reverses for larger ellipsoids. For high-curvature shapes, the surfactant tail has to adopt conformations with several gauche defects to ensure that it remains inside the micelle-core volume. Since the energy associated with a gauche defect is higher for a fluorocarbon chain than for a hydrocarbon chain,[28,29,31] fluorocarbon chains packed in a high-curvature geometry have a higher g_{pack} value compared with their hydrocarbon analogues.

3.3. Results for the Steric Free Energy of Biaxial Ellipsoidal Micelles. Figure 8 shows the variation of the local steric free energy per molecule, $g_{st,local}$, along the surface of an oblate ellipsoid. Similar to Figure 3, the curves are obtained by dividing eq 22 by eq 10 for an oblate ellipsoidal micelle formed by a six-carbon fluorocarbon surfactant with a tail volume of 292.0 Å^3, a_h = 50.0 Å^2, which is similar to the head area of a maltoside head (52.0 Å^2), and q = 7.40 Å, which is equal to 95% of the length of the six-carbon fluorocarbon tail. $g_{st,local}$ increases as the equatorial region located at $\nu = \pi/2$ is approached. This

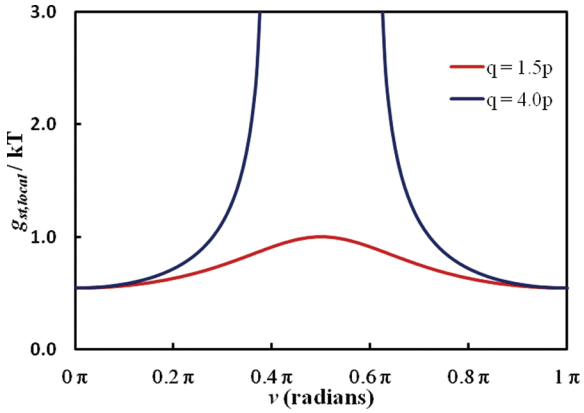

Figure 8. Variation of the local steric free energy per molecule, $g_{st,local}$, as a function of the angle ν.

follows because the area per molecule decreases as one moves from the polar region, located at $\nu = 0$ and π, to the equatorial region, located at $\nu = \pi/2$. The change in $g_{st,local}$ is more pronounced at high aspect ratios. In fact, beyond a threshold aspect ratio, the local steric free energy becomes infinite because the available surface area per molecule near the equatorial region is smaller than the head area of the surfactant. This is shown in the blue curve in Figure 8, which corresponds to an aspect ratio of 4.0. Therefore, similar to the theoretical limit on the size of ellipsoidal micelles established based on the interfacial free energy, we can derive a theoretical limit based on the steric free energy as follows:

$$1 - \frac{na_h}{4\pi p\sqrt{p^2\cos^2\nu + q^2\sin^2\nu}} > 0, \qquad 0 \le \nu \le \pi$$

$$\Rightarrow 4\pi p\sqrt{p^2\cos^2\nu + q^2\sin^2\nu} > (V/V_{tail})a_h, \quad 0 \le \nu \le \pi$$

$$\Rightarrow \begin{cases} q < \dfrac{3V_{tail}}{a_h}, & p < q \\ p < \dfrac{3V_{tail}}{a_h}, & p > q \end{cases} \tag{25}$$

Note that the only difference in the final result obtained in eq 25 from that obtained in eq 24 is the replacement of the shielding area per molecule, a_0, by the surfactant head area, a_h. Combining the two limits yields the following equation for the theoretical limit on the size of biaxial ellipsoidal micelles based on our molecular model.

$$q < \min\left(\frac{3V_{tail}}{a_h}, \frac{3V_{tail}}{a_0}\right), \quad p < q$$

$$p < \min\left(\frac{3V_{tail}}{a_h}, \frac{3V_{tail}}{a_0}\right), \quad p > q \tag{26}$$

Similar to Figure 4, the variation of the average steric free energy per molecule, g_{st}, as a function of the size of the ellipsoidal micelle for the same six-carbon fluorocarbon surfactant used to plot Figure 8 is shown in Figure 9. Comparison of Figures 4 and 9 shows that the trends observed for g_{st} are opposite to those observed for g_{int}. This follows because, while g_{int} increases with increasing surface area per molecule, g_{st} decreases with increasing surface area per molecule. However, it

dx.doi.org/10.1021/jp3012975 | J. Phys. Chem. B 2012, 116, 6443−6454

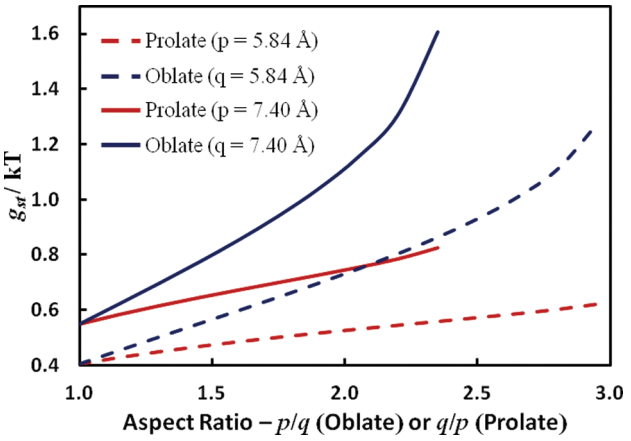

Figure 9. Variation of g_{st} with the aspect ratio of prolate ellipsoidal micelles and oblate ellipsoidal micelles. The dashed lines and the solid lines correspond to ellipsoidal micelles with semiminor axis length equal to 75 and 95% of the six-carbon fluorocarbon tail length, respectively. Note that, based on the condition derived in eq 25, the theoretical limit on the length of the semimajor axis (q for prolate ellipsoids and p for oblate ellipsoids) is 17.52 Å, and as a result, the solid curves extend only until an aspect ratio of 2.37.

is important to note that the magnitude of the difference between g_{st} of a prolate and an oblate ellipsoidal micelle is quite small compared to the magnitude of the difference between the g_{int} values. This suggests that the interfacial free-energy contribution to the micellization free energy is more important than the steric free-energy contribution in determining the optimal micelle shape.

Finally, based on the above arguments and our understanding of Figure 5, we can conclude that g_{st} for a micelle formed by hydrocarbon-based surfactants will be higher than g_{st} for a micelle of identical size formed by fluorocarbon-based surfactants having the same number of carbon atoms in the tail and the same head area. As stated in section 3.1, this trend can be attributed to the lower volume of hydrocarbon chains compared to that of fluorocarbon chains, leading to a lower surface area *per molecule*, and therefore to a higher g_{st}.

3.4. Shape Distribution of Micelles for Different Surfactants. To evaluate the feasibility of forming biaxial ellipsoidal micelles, we predicted the shape distribution of micelles formed by a six-carbon fluorocarbon-based nonionic surfactant (V_{tail} = 292.0 Å^3, σ_0 = 55.0 dyn/cm, δ = 1.28 Å, and a_0 = 29.8 Å^2) having a head area of 60 Å^2, at its CMC, in two different scenarios. In the first scenario, we assumed that micelles can exist in only three shapes, namely, spheres, spherocylinders (finite cylinders with hemispherical end-caps having the same radius as the cylinder), and discs (finite bilayers with semitoroidal rims[26]). In the second scenario, we assumed that micelles can exist in five shapes, namely, spheres, spherocylinders, discs, prolate ellipsoids, and oblate ellipsoids. The shape distribution for each of the scenarios was predicted by calculating the total number of surfactant molecules forming micelles of a particular shape using eq 3. The number of surfactant molecules forming a particular micelle of aggregation number, n, is given by $nX_n(N_W + N_S)$. Note that, in actual micellar systems, no restrictions can be imposed on the shapes that micelles can take. However, when modeling the micellization behavior of surfactants, micelle shapes are limited by the shapes that can be actually modeled in the context of a given computational framework. For example, some computational frameworks assume that the micelles are spherical, spherocylindrical, or disk-like in shape.[26] Our aim here is to show the effect of the modeling limitations on the model predictions.

The shape distributions corresponding to the two scenarios are shown in Figures 10 and 11. In the first scenario shown in

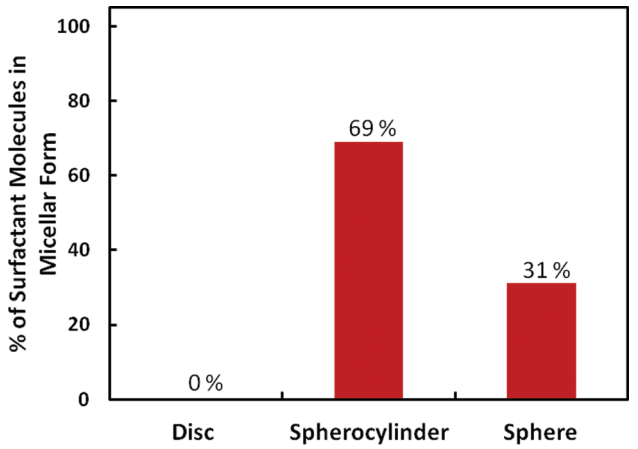

Figure 10. Shape distribution of micelles in the scenario where they can adopt spherical, spherocylindrical, and discoidal shapes.

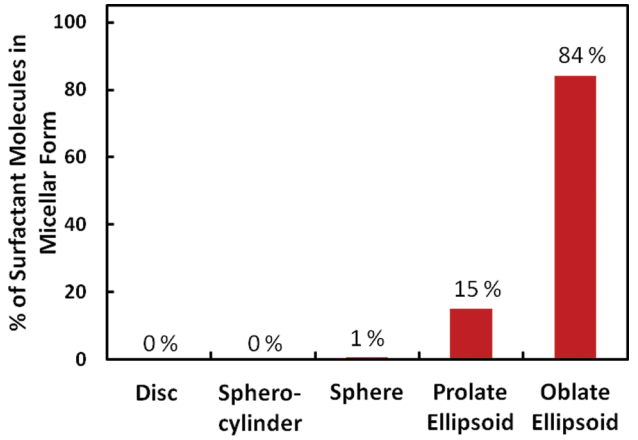

Figure 11. Shape distribution of micelles in the scenario where they can adopt spherical, spherocylindrical, discoidal, prolate ellipsoidal, and oblate ellipsoidal shapes.

Figure 10, 69% of the surfactant molecules in the micellar state form spherocylindrical micelles, while the remaining 31% form spherical micelles. The weight-average aspect ratio $\langle AR\rangle_W$ of the cylindrical micelles is 4.3, while that of the entire micellar solution (including cylindrical and spherical micelles) is 3.2. Here, the aspect ratio of a cylinder is defined as $(h + 2r)/2r$, where h is the height of the cylinder and r is the radius of the cylinder. The aspect ratio for a sphere is 1. The weight average of the aspect ratio is calculated using the following expression:

$$\langle AR\rangle_W = \frac{\sum_{n>1} AR \cdot nX_n}{\sum_{n>1} nX_n} \quad (27)$$

Using a definition which is similar to that of the weight-average aspect ratio, the weight-average aggregation number was calculated to be 39.

In the second scenario (Figure 11), where we have also allowed the formation of ellipsoidal micelles, we find that 84%

dx.doi.org/10.1021/jp3012975 | J. Phys. Chem. B 2012, 116, 6443−6454

of the surfactant molecules in the micellar state form oblate ellipsoidal micelles, 15% form prolate ellipsoidal micelles, and only 1% of the surfactant molecules in the micellar state form spherical, spherocylindrical, and discoidal micelles. Contrary to claims made in several theoretical studies,[10,13−15] this result clearly suggests that, in the context of our theoretical framework, ellipsoidal micelles are indeed feasible micelle shapes when compared with spheres, spherocylinders, and discs. The weight-average aggregation number and aspect ratio of the micelles are 13 and 1.23, respectively, which suggests that the micelles are globular and not very elongated.

Of all the five shapes considered, we found that an infinite cylinder of radius 8.54 Å has the lowest free energy of micellization of −8.81 kT. The next lowest free energy of micellization of −8.54 kT corresponds to an oblate ellipsoidal micelle of aggregation number 21 having a semiminor axis-length equal to 9.14 Å. This observation, along with the results shown in Figure 11, shows that, in spite of having a higher micellization free energy, the oblate ellipsoidal shape is the preferred shape. This can be attributed to two factors. First, in practice, only finite-size micelles can exist in solution, and in this case, the free energy associated with forming the spherical end-caps of a spherocylindrical micelle is significantly higher than that associated with forming the cylindrical portion. As a result, shorter spherocylinders have a much higher micellization free energy than longer spherocylinders. Second, the entropic penalty associated with localizing n surfactant monomers to form a surfactant micelle of aggregation number n is not included in the definition of the free energy of micellization introduced in eq 4. Instead, it is included while calculating the concentration of micelles using eq 3. This entropic penalty is smallest for small micelles and increases as the micelle aggregation number increases. As a result, at low concentration, when fewer surfactant molecules are available to form micelles, smaller micelles are preferred. Due to these two reasons, in the case considered above, oblate ellipsoids are the preferred shape in spite of having a higher free energy of micellization compared to an infinite cylindrical micelle. However, it should be noted that it is not impossible for an ellipsoidal micelle to have a free energy of micellization which is lower than that for the three regular shapes. In fact, for certain surfactants, we have seen that an oblate ellipsoidal shape has a lower free energy of micellization than that of a spherical, infinite cylindrical, or infinite bilayer micelle. Therefore, although the free energy of micellization per molecule varies with position for ellipsoidal micelles, its average value can still be sufficiently low to make it the preferred micelle shape.

Comparison of Figures 10 and 11 shows that the preference of spherocylinders over spheres in Figure 10 is reversed in Figure 11. To understand this trend reversal, we first note that all the predictions are made at the predicted surfactant CMC, defined as the surfactant concentration at which 95% of the surfactant molecules are dispersed as monomers and the rest form micelles.[32] On the basis of Figure 11, we note that the oblate ellipsoidal shape is the preferred micelle shape, and therefore, it is easier to form micelles in the second scenario compared to the first scenario. This lowers the CMC and, in turn, the monomer concentration in the second scenario, which favors the formation of smaller aggregates (spherical over spherocylindrical) due to the power-law dependence of X_n on X_1, as shown in eq 3. As a result, compared to Figure 10, the preference for spherocylinders over spheres is reversed in Figure 11.

Next, we compare the shape distribution of micelles as we change the numerous molecular descriptors of the micelle by varying (i) the tail length of the surfactant (by changing the number of carbon atoms in the surfactant tail), (ii) the surfactant head area, and (iii) the chemistry of the surfactant tail. Figure 12 shows the shape distribution of micelles at the CMC for a series of fluorocarbon-based surfactants having a head area of 60.0 Å^2, and five (V_{tail} = 250.4 Å^3, σ_0 = 55.0 dyn/cm, δ = 1.11 Å, and a_0 = 29.8 Å^2), six (V_{tail} = 292.0 Å^3, σ_0 = 55.0 dyn/cm, δ = 1.28 Å, and a_0 = 29.8 Å^2), and seven (V_{tail} = 333.6 Å^3, σ_0 = 55.0 dyn/cm, δ = 1.45 Å, and a_0 = 29.8 Å^2) carbon atoms in the tail. The figure shows no discernible difference between the shape distributions of micelles for the three different surfactants considered. The weight-average aspect ratio does not show a lot of variation either, with values between 1.23 and 1.27 for the three surfactants considered. This follows because, with an increase in the number of carbon atoms in the tail of the fluorocarbon-based surfactant, not only does the volume of the surfactant tail increase, but also the length of the semiminor axis of the ellipsoidal micelle increases. These two factors offset each other, leading to shape distributions that are very similar for the three different surfactants considered. The weight-average aggregation number increases from 10 to 19 as the length of the surfactant tail is increased.

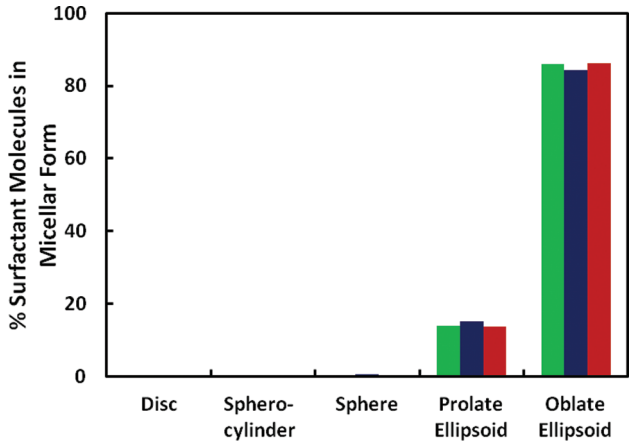

Figure 12. Shape distribution of micelles at the CMC of a series of fluorocarbon-based surfactants having different numbers of carbon atoms in the tail. Color code: green, five-carbon fluorocarbon tail; blue, six-carbon fluorocarbon tail; red, seven-carbon fluorocarbon tail.

In Figure 13, we compare the effect of the head area on the shape distribution of micelles at the surfactant CMC. Specifically, the figure shows the shape distribution of micelles at the CMC for three fluorocarbon-based surfactants with a six-carbon fluorocarbon tail having head areas of 50.0, 60.0, and 70.0 Å^2. Figure 13 shows that, as the head area increases, the fraction of surfactant molecules in the micellar state that form oblate ellipsoidal micelles decreases from 95 to 72%, while that for prolate ellipsoidal micelles increases from 4 to 27%. The weight-average aggregation number decreases from 20 to 9. In addition, the calculated weight-average aspect ratio decreases from 1.42 to 1.15; i.e., the micelles become increasingly globular. For this set of surfactants, the length of the surfactant tail remains the same. As a result, the semiminor axis length of the micelle also remains the same (at about 90−100% of he surfactant tail length). However, the head area increases.

dx.doi.org/10.1021/jp3012975 | J. Phys. Chem. B 2012, 116, 6443−6454

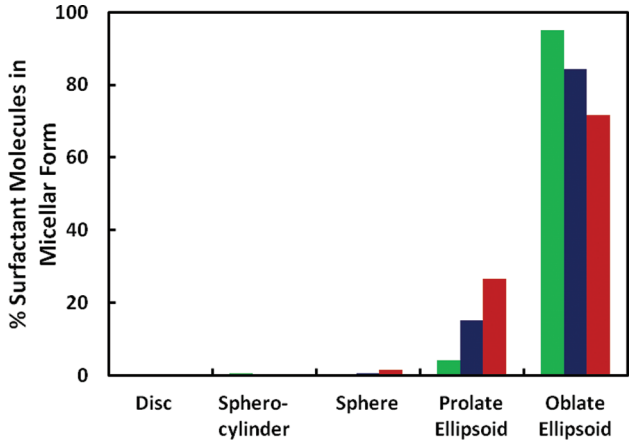

Figure 13. Shape distribution of micelles at the CMC of a series of six-carbon fluorocarbon-based surfactants having different head areas. Color code: green, 50.0 Å^2; blue, 60.0 Å^2; red, 70.0 Å^2.

Consequently, the steric repulsions between the heads increase, leading to a more globular-shaped micelle which has a higher surface area per volume ratio. Note that the increase in the contribution of the prolate ellipsoidal shape is also due to the same reason, since, for the same semiminor axis length and aspect ratio, a prolate ellipsoid has a higher surface area per molecule than an oblate ellipsoid.

The final plot in this section shown in Figure 14 compares the shape distribution of micelles formed by a six-carbon

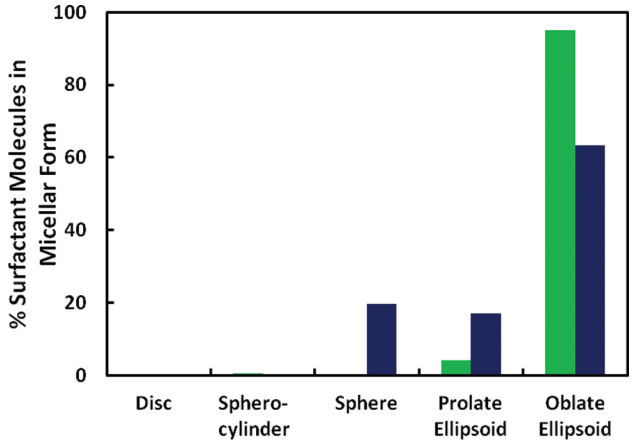

Figure 14. Shape distribution of micelles at the CMC of a six-carbon fluorocarbon-based surfactant (green) and a six-carbon hydrocarbon-based surfactant (blue), both having a head area of 50.0 Å^2.

fluorocarbon-based surfactant (V_{tail} = 292.0 Å^3, σ_0 = 55.0 dyn/cm, δ = 1.28 Å, and a_0 = 29.8 Å^2) and a six-carbon hydrocarbon-based surfactant (V_{tail} = 188.8 Å^3, σ_0 = 50.46 dyn/cm, δ = 1.19 Å, and a_0 = 21.0 Å^2) having the same head area of 50.0 Å^2. For the fluorocarbon-based surfactant, 95% of the surfactant molecules in the micellar state form oblate ellipsoidal micelles. On the other hand, for the hydrocarbon-based surfactant, about 63, 17, and 20% of the surfactant molecules in the micellar state form oblate ellipsoidal, prolate ellipsoidal, and spherical micelles, respectively. The calculated weight-average aspect ratio for the fluorocarbon-based surfactant micelles is 1.42, while that for the hydrocarbon-based surfactant micelles is 1.12. Consequently, the weight-average aggregation number for the fluorocarbon-based surfactant micelle is 20, while that for the hydrocarbon-based surfactant micelle is 11. These results can be explained on the basis of the volume of the two surfactant tails. Since the fluorocarbon tail is bulkier compared to the hydrocarbon tail, the fluorocarbon-based surfactant prefers to micellize in a shape having a higher volume-to-surface area ratio. Since an oblate ellipsoidal shape has a higher volume-to-surface area ratio, the fluorocarbon-based surfactant prefers to micellize in this shape more than its hydrocarbon analogue.

Finally, based on the results presented in Figures 11−14, it follows that, for the set of surfactants studied here, out of the two biaxial ellipsoidal shapes, oblate ellipsoids are preferred over prolate ellipsoids. This follows because, at a semiminor axis length of 95% of the surfactant tail length (which is representative of the preferred value), the oblate ellipsoidal shape is the preferred shape from an interfacial free-energy viewpoint, while the prolate ellipsoidal shape is the preferred shape from the steric free-energy viewpoint (the packing free energies are not very different for the two shapes). However, as stressed in section 3.3, the difference in the interfacial free energies of the two shapes is much higher than the difference in the steric free energies. As a result, the shape with the lower interfacial free energy, the oblate ellipsoidal shape in this case, becomes the preferred micelle shape. Note that, with an increase in the head area, the difference in the steric free energies of the two ellipsoidal shapes becomes increasingly significant, and this can lead to a change in the preferred shape from an oblate ellipsoidal to a spherical/prolate ellipsoidal shape. Furthermore, if the surfactants are ionic, there would be an additional electrostatic free-energy penalty, which may have a larger effect on the micelle shape distribution than that of the steric free energy.

4. CONCLUSIONS

In conclusion, we presented the first rigorous theoretical treatment based on molecular thermodynamics to calculate the free energy of micellization for biaxial ellipsoidal micelles. In our model, we incorporated the effects of the position-dependent curvature associated with the ellipsoidal shape to calculate the average micellization free energy per molecule. We have shown that, although the free energy of micellization for these micelle shapes has a position dependence, the average free energy of micellization can indeed be smaller than the free energy of micellization of the regular shapes, namely, spheres, infinite cylinders, and infinite bilayers. In addition, we also showed that a biaxial ellipsoidal shape can indeed be a feasible micelle shape compared to shapes like spheres, spherocylinders, and discs.

We derived theoretical limits on the size of the biaxial ellipsoidal micelles purely based on the molecular descriptors associated with the surfactant, namely, the surfactant tail volume, the head area, etc. We also showed that, for the surfactants considered here, the interfacial free-energy contribution to the free energy of micellization has a stronger effect on the micelle shape distribution. As a result, all the surfactants considered here prefer to form oblate ellipsoidal micelles rather than prolate ellipsoidal micelles. However, this could change for surfactants having a very bulky headgroup or an ionic head.

■ ASSOCIATED CONTENT

Supporting Information

Details of the implementation of the mean-field, statistical-mechanical method to calculate the packing free energy

dx.doi.org/10.1021/jp3012975 | J. Phys. Chem. B 2012, 116, 6443−6454

(section 1). Packing polynomials to calculate the packing free energy (section 2). This material is available free of charge via the Internet at http://pubs.acs.org.

AUTHOR INFORMATION

Corresponding Author

*Phone: 617-253-4594. Fax: 617-252-1651. E-mail: dblank@mit.edu.

Notes

The authors declare no competing financial interest.

ACKNOWLEDGMENTS

The authors are thankful to the DuPont-MIT Alliance for financial support. In addition, they thank Jonathan Mendenhall for providing useful feedback.

REFERENCES

(1) Porte, G. In *Micelles, Membranes, Microemulsions, and Monolayers*; Gelbart, W. M., Ben-Shaul, A., Roux, D., Eds.; Springer-Verlag: New York, 1994; pp 106−107.
(2) Attwood, D.; Florence, A. T. *Surfactant systems: Their chemistry, pharmacy and biology*; Chapman and Hall: New York, 1983; 80−87, 260−263, 282−283.
(3) Clint, J. H. *Surfactant Aggregation*; Chapman and Hall: New York, 1992; pp 85−98.
(4) Tanford, C.; Nozaki, Y.; Rohde, M. F. *J. Phys. Chem.* **1977**, *81*, 1555−1560.
(5) Kawaguchi, T.; Hamanaka, T.; Kito, Y.; Machida, H. *J. Phys. Chem.* **1991**, *95*, 3837−3846.
(6) Caetano, W.; Gelamo, E. L.; Tabak, M.; Itri, R. *J. Colloid Interface Sci.* **2002**, *248*, 149−157.
(7) Sarkar, B.; Lam, S.; Alexandridis, P. *Langmuir* **2010**, *26*, 10532−10540.
(8) Bogusz, S.; Venable, R. M.; Pastor, R. W. *J. Phys. Chem. B* **2000**, *104*, 5462−5470.
(9) Tieleman, D. P.; van der Spoel, D.; Berendsen, H. J. C. *J. Phys. Chem. B* **2000**, *104*, 6380−6388.
(10) Israelachvili, J. N.; Mitchell, D. J.; Ninham, B. W. *J. Chem. Soc., Faraday Trans. 2* **1976**, *72*, 1525−1568.
(11) Tartar, H. V. *J. Phys. Chem.* **1955**, *59*, 1195−1199.
(12) Tanford, C. *J. Phys. Chem.* **1972**, *76*, 3020−3024.
(13) Leibner, J. E.; Jacobus, J. *J. Phys. Chem.* **1977**, *81*, 130−135.
(14) Taddei, G. *Colloid Polym. Sci.* **1994**, *272*, 1300−1305.
(15) Taddei, G. *J. Chem. Soc., Faraday Trans.* **1993**, *89*, 1749−1751.
(16) Halle, B.; Landgren, M.; Jönsson, B. *J. Phys. (Paris)* **1988**, *49*, 1235−1259.
(17) Nagarajan, R.; Ruckenstein, E. *Langmuir* **1991**, *7*, 2934−2969.
(18) Borkovec, M. *Adv. Colloid Interface Sci.* **1992**, *37*, 195−217.
(19) Puvvada, S.; Blankschtein, D. *J. Chem. Phys.* **1990**, *92*, 3710−3724.
(20) Blankschtein, D.; Thurston, G. M.; Benedek, G. B. *Phys. Rev. Lett.* **1985**, *54*, 955−958.
(21) Nagarajan, R. *Colloids Surf., A* **1993**, *71*, 39−64.
(22) Shiloach, A.; Blankschtein, D. *Langmuir* **1998**, *14*, 1618−1636.
(23) Abraham, M. H. *J. Chem. Soc., Faraday Trans. 1* **1984**, *80*, 153−181.
(24) Tolman, R. C. *J. Chem. Phys.* **1949**, *17*, 333−337.
(25) Ben-Shaul, A.; Szleifer, I.; Gelbart, W. M. *J. Chem. Phys.* **1985**, *83*, 3597−3611.
(26) Srinivasan, V.; Blankschtein, D. *Langmuir* **2005**, *21*, 1647−1660.
(27) Millman, R. S., Parker, G. D. *Elements of Differential Geometry*; Prentice-Hall: Englewood Cliffs, NJ, 1977; pp 74−136.
(28) Flory, P. J. *Statistical Mechanics of Chain Molecules*; Hanser Publishers: New York, 1969; pp 133−157.
(29) Mattice, W. L., Suter, U. W. *Conformational Theory of Large Molecules: The Rotational Isomeric State Model in Macromolecular Systems*; Wiley: New York, 1994; 52−66, 143−152.
(30) Naor, A.; Puvvada, S.; Blankschtein, D. *J. Phys. Chem.* **1992**, *96*, 7830−7832.
(31) Bates, T. W.; Stockmayer, W. H. *J. Chem. Phys.* **1966**, *45*, 2321−2322.
(32) Tanford, C. *The Hydrophobic Effect: Formation of Micelles and Biological Membranes*; John Wiley & Sons, Inc.: New York, 1980; pp 63−77.